Heliyon 8 (2022) e10151

Contents lists available at ScienceDirect

Heliyon

journal homepage: www.cell.com/heliyon

Research article

X-ray structure, hirshfeld surfaces and interaction energy studies of 2,2-diphenyl-1-oxa-3-oxonia-2-boratanaphthalene

N.R. Sreenatha [a,b], D.P. Ganesha [a], A.S. Jeevan Chakravarthy [c], B. Suchithra [d], B.N. Lakshminarayana [a,*]

[a] Department of Engineering Physics, Adichunchanagiri Institute of Technology, Chikkamagaluru, 577 102, Karnataka, India
[b] Department of Physics, Government Engineering College, Hassan, 573 201, Karnataka, India
[c] New Chemistry Unit (NCU), JNCASR, Amruthahalli, Bangalore, 560064, Karnataka, India
[d] Department of Biochemistry, Maharani Science College for Women, Bengaluru, 560 001, Karnataka, India

GRAPHICAL ABSTRACT

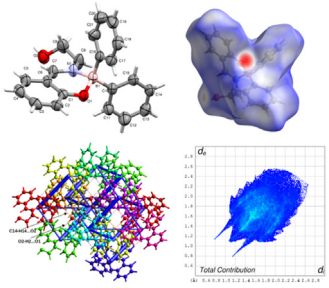

ARTICLE INFO

Keywords:
Single crystal XRD
Boratanaphthalene
Intermolecular interactions
Hirshfeld surfaces
3D-interaction energies

ABSTRACT

Single crystal XRD structure of the title compound reveals that the molecule adopt non-planar structure. The molecule is puckered with the total puckering amplitude of (Q) = 0.368(3)Å. Crystals of the title molecules are interconnected by intermolecular O–H···O and C–H···O interactions to develop 1D chains extending infinitely along the crystallographic *a*-axis. The intermolecular interactions were explored by Hirshfeld surfaces and their associated fingerprint graphs are obtained which revealed that the H···H and H···C pairs of inter atomic contacts were pre-dominant in the crystal packing of title compound. The energy of intermolecular interactions are computed using the accurate energy density model of B3LYP/6–31 G(d,p).

* Corresponding author.
E-mail addresses: bnlphysics@gmail.com, lakshminarayanabn@aitckm.in (B.N. Lakshminarayana).

https://doi.org/10.1016/j.heliyon.2022.e10151
Received 15 January 2022; Received in revised form 12 April 2022; Accepted 27 July 2022

Specification Table

Subject area	X-ray crystallography
Compound	2,2-Diphenyl-1-oxa-3-oxonia-2-boratanaphthalene
Data category	Crystallographic data
Data acquisition format	CIF
Data type	Analysed
Procedure	Crystal structure determination, interpretation and computational analysis
Data accessibility	CCDC: 2064704

1. Introduction

Boron fused tri- and tetra-coordinated molecules have found great importance for multifunctional applications such as OLEDs, bio-imaging etc. due to their wide window of electronic properties. Some of the tetra-coordinated boron chelated N, O structures have found to be highly emissive in solid state with colour tunability due to their rigid π-conjugated structures [1, 2]. Crystal structure and molecular packing play major role in the light emissive devices wherein weak π···π interactions greatly helps for enhanced emission [3]. Hence understanding the structural dynamics of the molecule is of great significance in this perspective. The literature study strongly reveals that, the organic compounds bearing hetero atoms possess significant biological activities such as anti-viral, anti-fungal, anti-cancer, etc. [4, 5, 6] Further, presence of inter-molecular interactions in the architecture of crystal packing and their co-operation with hydrogen bonding guides in the synthetic and catalytic utility. Owing to this, the intermolecular interactions present in the crystal were investigated by three dimensional Hirshfeld surfaces (3D-HS) and also their energies were evaluated using accurate energy density wavefunction of B3LYP/6-31G(d,p). With respect to all the above perspectives and in continuation of our ongoing work on structural studies, we now report the structural and Hirshfeld surface studies of the compound 2,2-diphenyl-1-oxa-3-oxonia-2-boratanaphthalene.

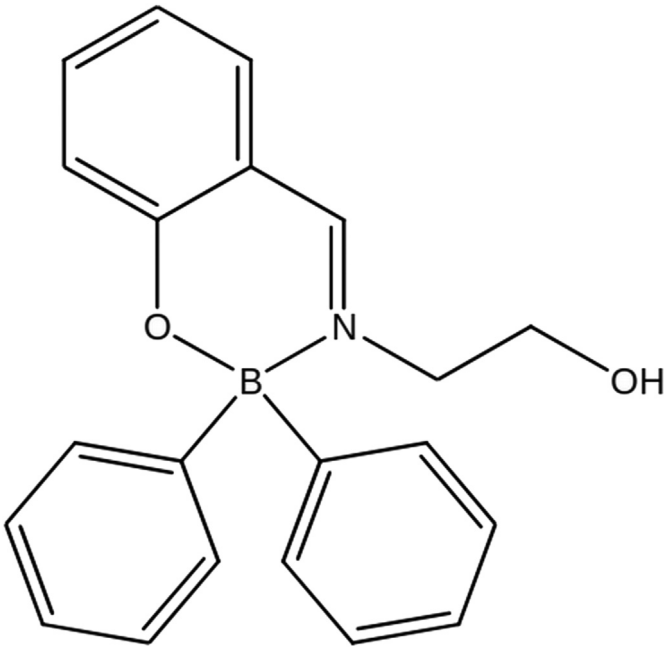

Figure 1. Schematic diagram of the compound 2,2-diphenyl-1-oxa-3-oxonia-2-boratanaphthalene.

2. Procedures

2.1. Experimental

2,2-Diphenyl-1-oxa-3-oxonia-2-boratanaphthalene was synthesized according to the reported procedure [7]. 2-(diphenylboryl)ethanamine (100 mg, 0.96 mmol) was refluxed with 2-hydroxybenzaldehyde (100μL, 0.96 mmol) in 5 mL methanol for 4 h to obtain cream colour solid with 90% yield (Figure 1). Single crystals were grown in ethanol using slow evaporation method.

2.2. Single crystal XRD

The structural and refinement details of the title compound are given in Table 1. A suitable size of block shaped single crystal was selected carefully for X-ray diffraction study. The diffraction data were collected on an Apex Bruker-II diffractometer equipped with MoKα radiation of wavelength 0.71073Å. Complete X-ray intensity data set was processed by SAINT software [8]. The crystal and molecular structure was solved by direct method using SHELXS and refined by full-matrix least squares based on F^2 SHELXL [9, 10, 11]. All the non-hydrogen atoms were refined anisotropically while the hydrogen atoms were refined isotropically and placed at chemically ideal positions with isotropic displacement parameters as C–H = 0.93Å with $U_{iso}(H) = 1.2U_{eq}(C)$ for aromatic rings and O–H = 0.82Å with $U_{iso}(H) = 1.5U_{eq}(O)$. The molecular and packing diagram were generated using the MERCURY [12] while PLATON software was used to obtain geometric parameters viz., bond distances, inter-bond angles and torsional angles [13, 14]

Table 1. Crystal, structural and refinement statistics.

CCDC	2064704
Chemical formula	$C_{21}H_{19}BNO_2$
Mr	328.18
Crystal system, space group	Monoclinic, *P21/n*
Temperature (K)	290
a, *b*, *c*, β (Å,°)	9.1024(6), 17.8682(15), 10.9790(9), 96.933(2)
V (Å^{-3}), Z	1772.6(2), 4
Radiation type	MoKα
μ (mm^{-1})	0.08
Crystal size (mm)	0.40 × 0.36 × 0.31
Diffractometer	*APEX (Bruker, 2006)*
No. of measured, independent and observed reflections	22044, 3649, 1990
R_{int}	0.05
$(\sin\theta/\lambda)_{max}$ (Å^{-1})	0.627
Goodness-of-Fit (S)	1.048
$R[F^2 > 2\sigma(F^2)]$, $wR(F^2)$, *S*	0.0632, 0.2065, 1.048
No. of reflections	3649
No. of parameters	226
Data/Restraints/Parameters	3649/0/226
H-atom treatment	H-atoms treated by a mixture of independent and constrained refinement
$\Delta\rho_{max}$, $\Delta\rho_{min}$ (eÅ^{-3})	0.55, -0.34
Index ranges	h = -11→10, k = -22→22, l = -13→13
Theta range (°)	Θmax = 25.2, θmin = 2.2

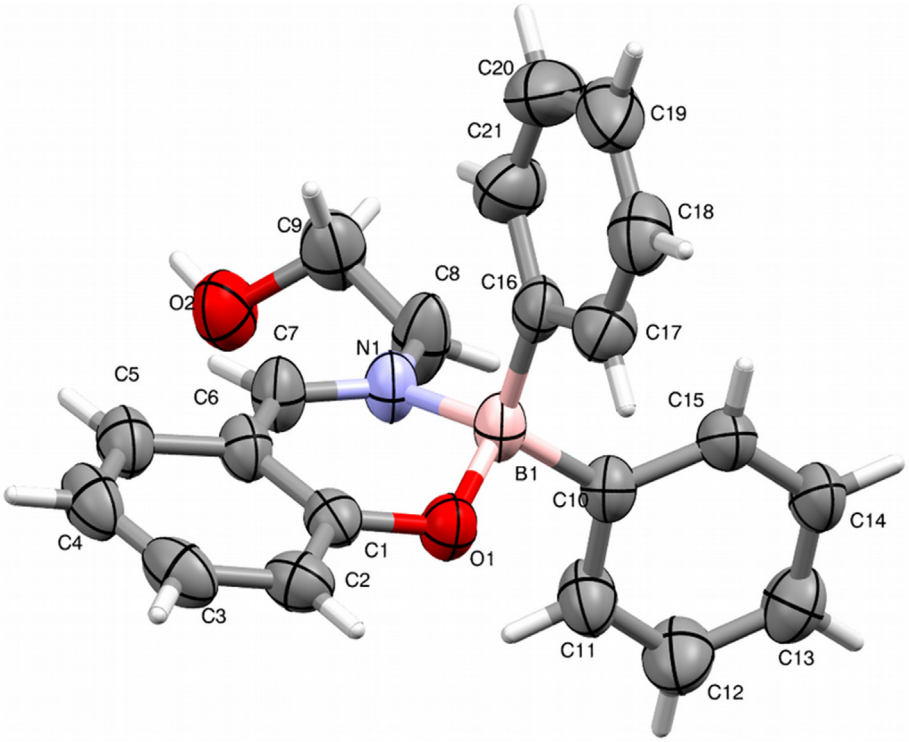

Figure 2. Thermal ellipsoids of a title molecule at 50% of probability.

2.3. Computational studies

Three dimensional Hirshfeld surfaces (3D-HS) mapped on both d_{norm} and electrostatic potentials (ESP), and their associated two dimensional fingerprint graphs are carried out making use of Crystal Explorer 17.5 software and to compute three dimensional interaction energies [15, 16, 17, 18, 19, 20]

3. Results and discussions

3.1. Structural commentary

The molecular structure of the title compound consists of a ten-membered heterocyclic ring [O1–B1–N1–C1/C7] and two phenyl rings [C10/C15] and [C16/C21] which are interlinked such that to have a non-coplanar view, and an -ethoxy group as an extended conformation as given in thermal ellipsoids drawn at 50% probability (Figure 2). The ten-membered ring [O1–B1–N1–C1/C7] displayed a puckering environment at B1 with the total puckering amplitude (Q) of 0.368 (3)Å and displayed a *half-chair* conformation. The pseudorotation (θ) and the relative phase (φ) angles are 114.0(3)° and 136.6 (4)° respectively [21, 22]

In the molecule, the mean planes of phenyl rings [(C10/C15) and (C16/C21)] are inclined with the dihedral angle of 77.05 (1)°. The central ten-membered ring (O1–B1–N1–C1/C7) makes the dihedral angle of 85.65(12)° and 87.55(1)° with the mean planes of phenyl rings (C10/C15) and (C16/C21) respectively, which reveals that the rings exhibits nearly an orthogonal relation to each other. The chain, N1–C8–C9–O2 adopts a *-syn-clinal conformation* with the torsional angle of -75.27°. The bond lengths and inter-bond angle values agree with the standard values [23, 24, 25, 26, 27, 28, 29].

3.1.1. Crystal packing

The crystal of the titled molecule are governed by an intermolecular O2–H2···O1 and C14–H14···O2 interactions (Table 2), to develop an independent 1D polymeric chains propagating indefinitely along crystallographic *a*-axis, as depicted in Figure 3. In addition to this, the titled molecule also comprise an intra-molecular C7–H7···O2 interaction, incorporating a self-assembly closed *S(6)* loop.

3.2. Computational analysis

The volume of 3D-HS mapped on d_{norm} (Figure 4) and electrostatic potential (Figure 5) are 369.88Å^2 and 435.97Å^3 respectively, with the colour scales of [−0.5324 a.u (red) and +1.4509 a.u (blue)], and [−0.1112 a.u (red) and +0.1478 a.u (blue)] respectively. The surfaces are given in transparent mode to understand the position of all the elements and the functional groups available in the molecule. The d_{norm} furnishes both the donor and acceptor regions of hydrogen bonding interactions by forming red colour circular spots on its surface with equal brightness.

For instance, the donor and acceptor regions of intermolecular O2–H2···O1 interaction can be viewed on the front and rear views of d_{norm} surfaces, given in Figures 4 a and b respectively. In Figure 4a the red spot surrounding O2–H2 and at the vicinity of O1 in Figure 4b are the indicators of donor and acceptor regions of O2–H2···O1 interaction (Table 2) [30, 31, 32, 33]. This is also substantiated by electrostatic

Table 2. Hydrogen bonding geometry (Å,°).

Interaction	D-H...A	d(H...A)	d(D...A)	Angle (D-H...A)	Symmetry code
Intra-molecular	C7–H7···O2	2.30	2.970(4)	129	
Intermolecular	O2–H2···O1	2.08	2.900(3)	176	*-1/2+x,1/2-y,1/2+z*
	C14–H14···O2	2.52	3.363(4)	152	*1+x,y,z*

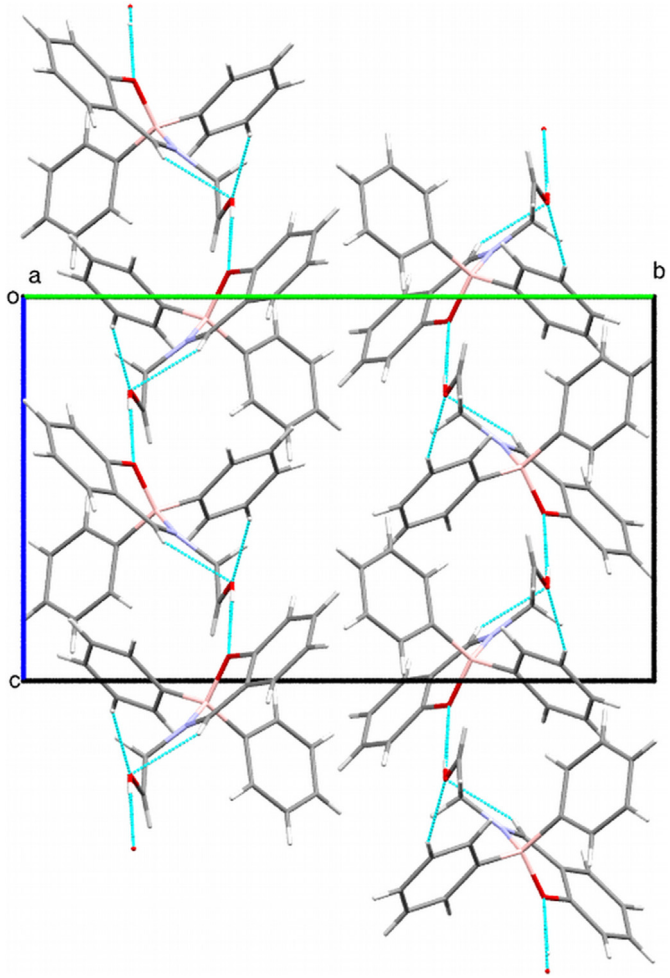

Figure 3. Packing of the title molecules when it is viewed along crystallographic *a*-axis.

potentials (Fig. 5a and b are front and rear views) by reflecting intense blue coloured patch around O2–H2, while the red coloured patch around O1 represents the electrostatic positive donor and negative acceptor potentials respectively. These electrostatic interactions serve as an important tool in the binding of protein targets [34].

The two-dimensional fingerprint graphs were generated in an expanded mode for all the major contacts, and it is delineated in Figure 6. Total contribution from all the pairs of inter atomic contacts is given in Figure 6(a). The highest contribution is represented by a pair of H···H inter atomic contacts with 60.9%, reflected as a pair of blue coloured spoke like pattern, merged almost in the middle of the graph at de + di = 1.1Å Figure 6(b). The 29.9% of contribution was made to the Hirshfeld surface from H···C pair of inter atomic contacts producing a pair of unique blue coloured wings between the region of 1.12Å<(de + di) < 1.72Å Figure 6(c). The pair of H···O inter atomic contacts represents only 7.9% of total contribution which is emerged as a characteristic sharp spikes over the region of 0.79 Å<(de + di) < 1.18Å Figure 6(d). Presence of H···O and H···C contacts correlates with the intermolecular interactions given in Table 2. Lastly, the C···C inter atomic contacts comprise only 2.2% to the crystal packing which is observed as an arrowhead pattern in the region of de + di ≈ 1.70Å pointing diagonally left downwards Figure 6(e). Overall study of fingerprint graphs reveals that the pair of H···H and H···C inter atomic contacts are the predominant ones. While H···O and C···C contacts are less significant in the formation of a three dimensional Hirshfeld surface.

Three-dimensional interaction energies were computed for the title compound using the CrystalExplorer17.5 software [35, 36]. Interaction energy was calculated using an accurate energy density model of B3LYP/6-31G(d,p), during the calculation a cluster of seventeen molecules (comprising a total of 748 atoms) of various colour coding scheme from different Cartesian co-ordinates were surrounding the original one (showed by black coloured ball and stick model) within the default radius of 3.8Å. The total interaction energy (E_{tot}) in the energy framework have been classified into classic electrostatic (E_{ele}), polarization (E_{pol}), dispersion (E_{dis}) and exchange repulsion (E_{rep}) energies [37].

Further, in the generation of electrostatic, dispersion and total energy frameworks, the tube size of 50 and threshold cut-off energy level of 10 kJ/mol were maintained. The Coloumbic (E_{ele}) energy terms are represented by red coloured solid cylinders (Figure 7), and green coloured solid cylinders in the construction of dispersion energy (E_{tot}) frameworks given in Figure 8. The total energy (E_{tot}) terms are constructed by using the blue coloured solid cylinders (Figure 9). In each of the energy profile the difference in thickness of solid cylinders reveals the relative strength of interaction with the constituent members of a cluster [38, 39], and plays an important role in the integrity of a crystal packing. Also, the red- and orange-coloured dashed lines in all the energy profiles reveal the molecules involved in the hydrogen bonding interactions given in Table 2. The total interacting energies in the cluster of title compound are given in component form (Table 3). Accordingly, the highest total interaction energy (E_{tot} = -67.6 kJ/mol from all the components) was noticed with a pair of symmetric pale-green coloured molecules interacting at the centroid distance of R = 7.76Å which correlates with the intermolecular O2–H2···O1 interaction. The total interaction energy

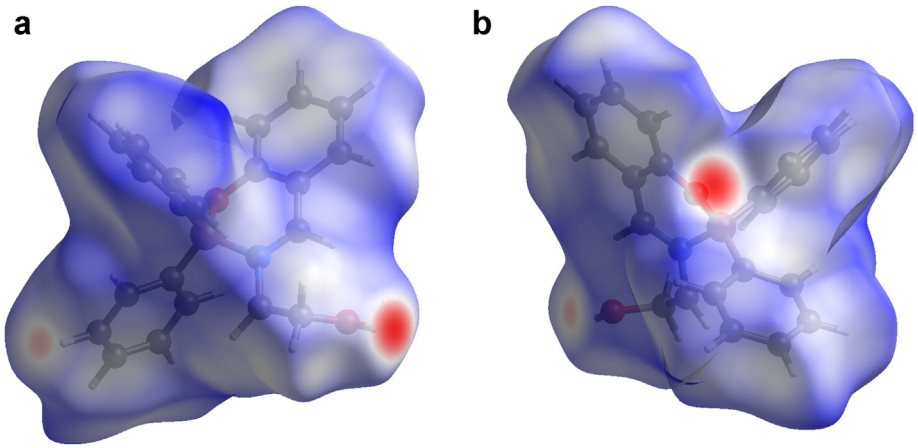

Figure 4. Front (a) and rear (b) views of Hirshfeld surface mapped on d_{norm}.

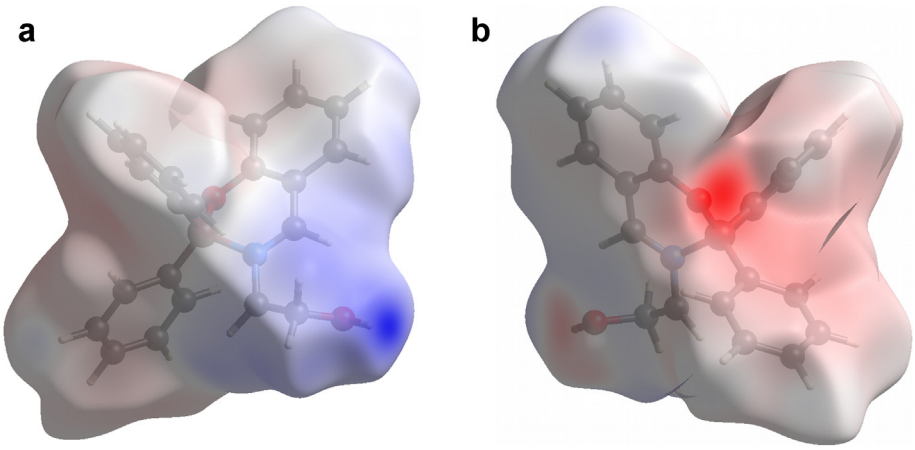

Figure 5. Front (a) and rear (b) views of HS mapped on electrostatic potentials.

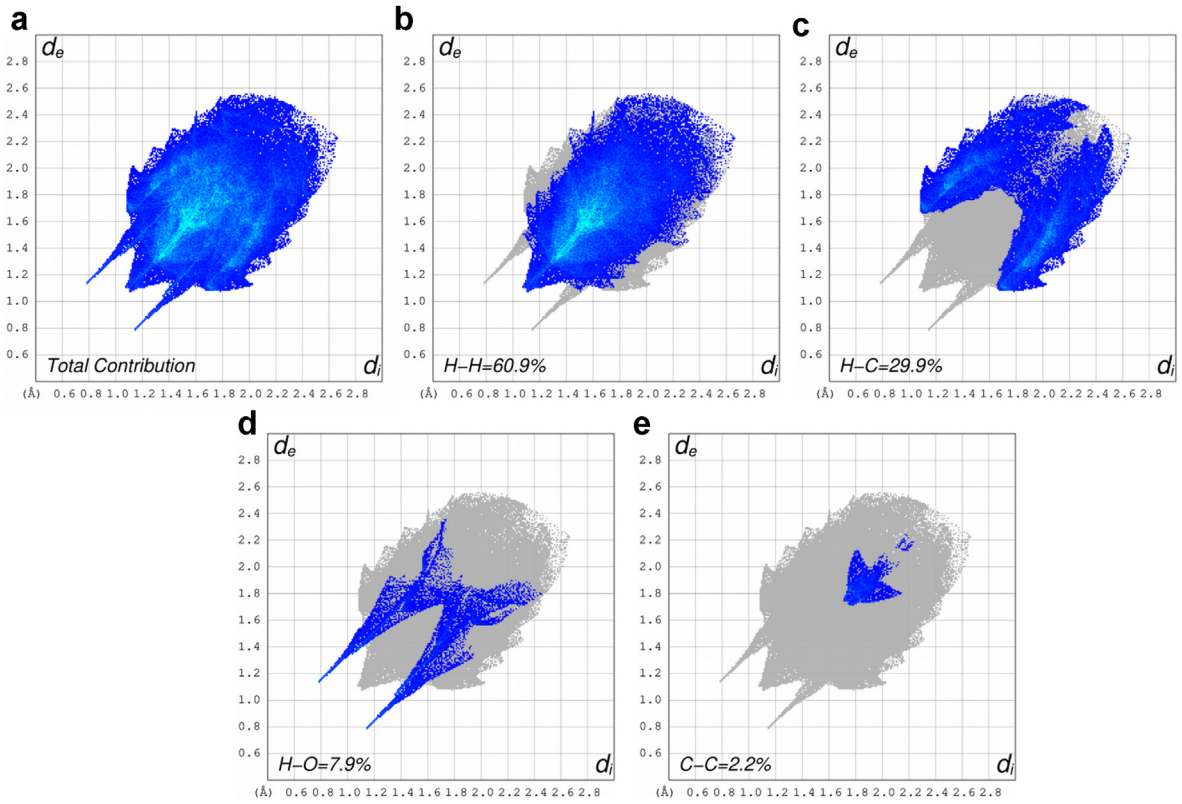

Figure 6. Two dimensional fingerprints graphs for the title compound. The di and de along *x* and *y* represents the nearest adjacent nuclei internal and external from the three dimensional Hirshfeld surface. (a) Total contribution, (b) H···H (c) H···C (d) H···O and (e) C···C inter atomic contacts.

(E_{tot} = -18.2 kJ/mol) associated with an intermolecular C14–H14···O2 interaction confirms with the red coloured molecules at the centroid distance of R = 9.10Å. The least total interaction energy was observed as E_{tot} = -1.8 kJ/mol associated with a couple of pink coloured molecules having the longest molecular centroid distance of R = 13.14Å. Further, the total energy from all the components in a cluster, the dispersion energy (E_{dis}) terms were dominated over the other terms as observed in the reported compounds [40, 41, 42]. Further, the total interaction energies are varying with the molecular centroid distances obeying the laws of electrostatics.

4. Conclusion

The title compound is crystallized in a monoclinic system with P21/n space group. The molecular structure of the compound was puckered at B1 and adopts *half-chair* conformation. The packing of molecules were governed by intra- and intermolecular C–H···O and O–H···O interactions and, they are explored by three dimensional Hirshfeld surfaces and fingerprint calculations, revealing that the H···H and H···C pairs of inter atomic contacts have made the significant contribution towards the formation of three dimensional

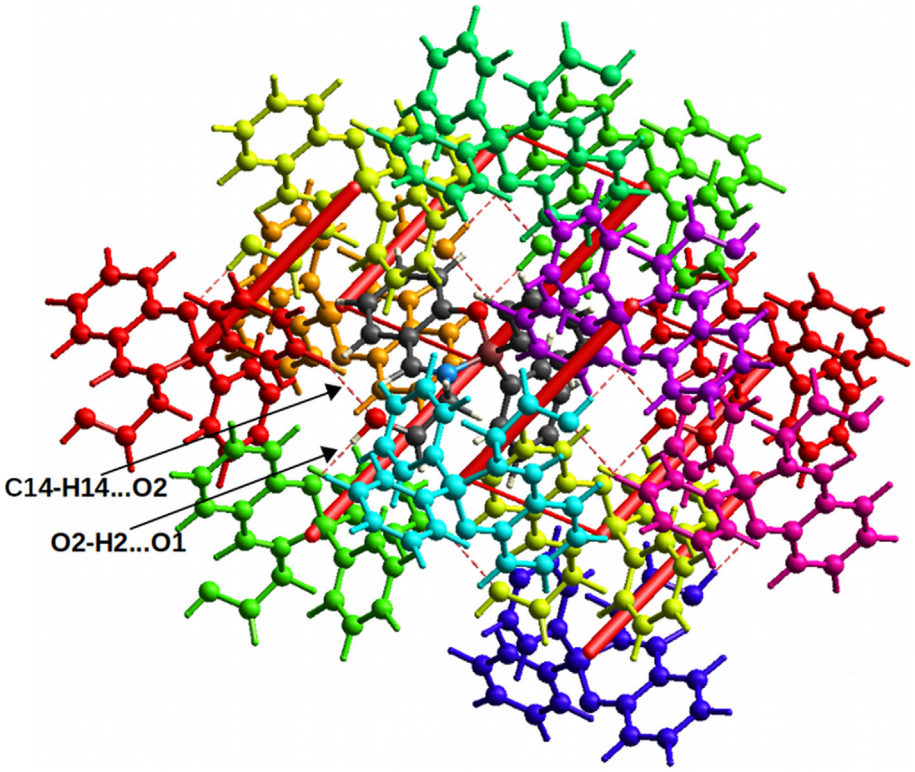

Figure 7. Three-dimensional interaction energy profile for Coloumbic (E_{ele}) terms generated with the tube size of 50 and cut-off energy of 10 kJ/mol for clarity purpose.

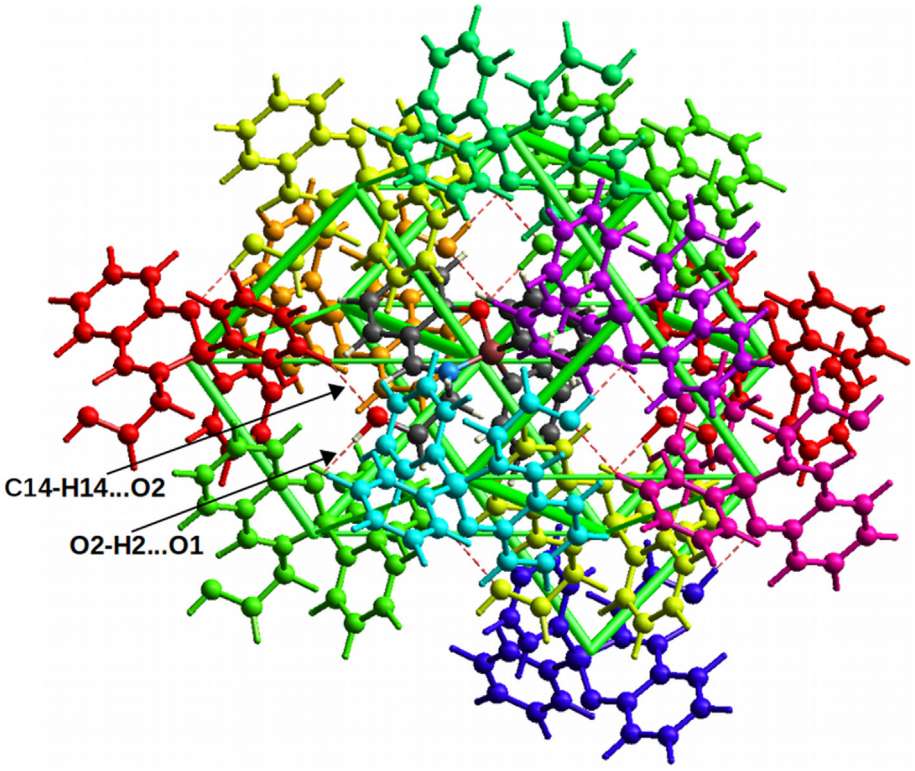

Figure 8. Three-dimensional interaction energy profile for dispersion (E_{dis}) terms generated with the tube size of 50 and cut-off energy of 10 kJ/mol for clarity purpose.

Hirshfeld surfaces. The interaction energy calculations reveal -67.6 kJ/mol is the highest total interaction energy (from all the components) associated with an intermolecular O2–H2···O1 interaction. Further, in the energy frameworks, in each case the dispersion energy E_{dis} term dominated over other components obeying laws of electrostatics.

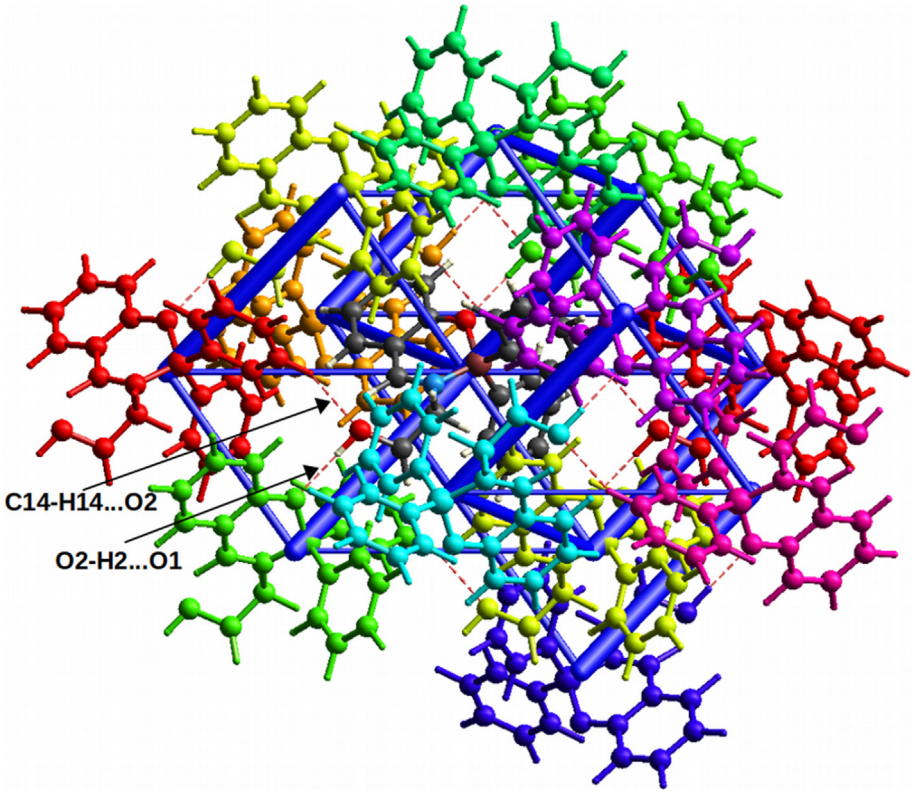

Figure 9. Three-dimensional interaction energy profile for total energy (E_{tot}) terms generated with the tube size of 50 and cut-off energy of 10 kJ/mol for clarity purpose.

Table 3. Three-dimensional interaction energies (kJ/mol) in component form for the title compound for *electron density B3LYP/6-31G(d,p)*. **Colour code:** Colour coding scheme of molecules, **N:** Number of interacting molecules with the reference one, **Symop**: Rotational symmetry operator, **R:** Molecular centroid distance. Scale factor: $E_{tot}= k_{ele}\ x\ E_{ele} + k_{pol}\ x\ E_{pol} + k_{dis}\ x\ E_{dis} + k_{rep}\ x\ E_{rep}$ Mackenzie et al. [43].

Colour code	N	Symop	R	E_{ele}	E_{pol}	E_{dis}	E_{rep}	E_{tot}
	2	x, y, z	9.10	-8.1	-1.7	-19.4	13.7	-18.2
	1	-x, -y, -z	8.40	-14.1	-3.6	-51.8	35.7	-40.7
	2	x+1/2, -y+1/2, z+1/2	6.94	0.2	-2.9	-42.4	18.2	-27.5
	2	x+1/2, -y+1/2, z+1/2	7.76	-46.6	-15.6	-44.3	51.5	-67.6
	2	-x+1/2, y+1/2, -z+1/2	11.41	-1.8	-0.3	-8.6	5.9	-6.0
	2	-x+1/2, y+1/2, -z+1/2	9.75	-2.4	-0.6	-8.4	1.3	-9.5
	1	-x, -y, -z	8.79	-0.9	-0.7	-18.6	7.8	-12.9
	1	-x, -y, -z	12.28	-0.7	-0.1	-4.8	1.6	-4.0
	1	-x, -y, -z	11.93	-0.9	-0.4	-8.4	2.8	-6.8
	2	-x+1/2, y+1/2, -z+1/2	13.14	0.1	-0.1	-2.4	0.2	-1.8

Declarations

Author contribution statement

N. R. Sreenatha: Analyzed and interpreted the data; Wrote the paper.
D. P. Ganesha: Contributed reagents, materials, analysis tools or data.
A. S. Jeevan Chakravarthy, B. N. Lakshminarayana: Conceived and designed the experiments.
B Suchithra: Performed the experiments.

Funding statement

This research did not receive any specific grant from funding agencies in the public, commercial, or not-for-profit sectors.

Data availability statement

Data associated with this study has been deposited at CCDC under the accession number 2064704.

Declaration of interests statement

The authors declare no conflict of interest.

Additional information

No additional information is available for this paper.

Acknowledgements

Authors are thankful to Dr. (Mrs) R. Chandramani, Professor (Rtd), Department of Physics, Bangalore University, Bengaluru (India) for her support, and Prof. M Jayashankar, St. Joseph's Autonomous College, Bengaluru, Karnataka, India. Dedicating to our Respected Professor (Rtd), Dr. (Mrs.) R. Chandramani, Ph.D, D.Sc., Bangalore University, and beloved N. S. Vedha Karthik, Hassan and A. J. Siddhanth Chakravarthy, Bangalore.

References

[1] D. Li, H. Zhang, C. Wang, S. Huang, J. Guo, Y. Wang, Construction of full-color-tunable and strongly emissive materials by functionalizing a boron-chelate four-ring-fused π-conjugated core, J. Mater. Chem. 22 (2012) 4319–4328.
[2] Y. Kubota, K. Kasatani, H. Takai, K. Funabiki, M. Matsui, Strategy to enhance solid-state fluorescence and aggregation-induced emission enhancement effect in pyrimidine boron complexes, Dalton Trans. 44 (2015) 3326–3341.
[3] S. Feng, S. Gong, G. Feng, Aggregation-induced emission and solid fluorescence of fluorescein derivatives, Chem. Commun. 56 (2020) 2511–2513.
[4] S.A. Patel, T. Rajale, E. O'Brien, D.J. Burkhart, J.K. Nelson, B. Twamley, A. Blumenfeld, M.I. Szabon-Watola, J.M. Gerdes, R.J. Bridges, N.R. Natale, Isoxazole analogues bind the system X_c-transporter: structure–activity relationship and pharmacophore model, Bioorg. Med. Chem. 18 (2010) 202–213.
[5] N.M. Silva, J.L.M. Tributino, A.L.P. Miranda, E.J. Barrerio Carlos, F.M. Fraga, New isoxazole derivatives designed as nicotinic acetylcholine receptor ligand candidates, Eur. J. Med. Chem. 37 (2002) 163–170.
[6] J. Kaffy, R. Pontikis, D. Carrez, A. Croisy, C. Monneret, J.-C. Florent, Isoxazole-type derivatives related to combretastatin A-4, synthesis and biological evaluation, Bioorg. Med. Chem. 14 (2006) 4067–4077.
[7] K.E. Claas, E. Hohaus, Pre-column fluorescent derivatization for high-performance liquid chromatography with 2,2-diphenyl-1-oxa-3-oxonia-2-boratanaphthalene (DOOB): determination of aminoalkanols, Z. für Anal. Chem. 322 (1985) 343–347.
[8] Bruker, APEX2 and SAINT, Bruker AXS Inc., Madison, Wisconsin, USA, 2006.
[9] G.M. Sheldrick, A short history of *SHELX*, Acta Crystallogr. A64 (2008) 112–122.
[10] G.M. Sheldrick, Crystal structure refinement with *SHELXL*, Acta Crystallogr. C71 (2015) 3–8.
[11] G.M. Sheldrick, *SHELXT* - Integrated space-group and crystal-structure determination, Acta Crystallogr. A71 (2015b) 3–8.
[12] C.F. Macrae, I. Sovago, S.J. Cottrell, P.T.A. Galek, P. McCabe, E. Pidcock, M. Platings, G.P. Shields, J.S. Stevens, M. Towler, P.A. Wood, *Mercury 4.0*: from visualization to analysis, design and prediction, J. Appl. Crystallogr. 53 (2020) 226–235.
[13] A.L. Spek, What makes a crystal structure report valid? Inorg. Chim. Acta. 470 (2018) 232–237.
[14] A.L. Spek, checkCIF validation ALERTS: what they mean and how to respond, Acta Crystallogr. E76 (2020) 1–11.
[15] M.A. Spackman, D. Jayatilaka, Hirshfeld surface analysis, CrystEngComm 11 (2009) 19–32.
[16] M.A. Spackman, J.J. McKinnon, Fingerprinting intermolecular interactions in molecular crystals, CrystEngComm 4 (2002) 378–392.
[17] M.A. Spackman, J.J. McKinnon, D. Jayatilaka, Electrostatic potentials mapped on Hirshfeld surfaces provide direct insight into intermolecular interactions in crystals, CrystEngComm 10 (2008) 377–388.
[18] J.J. McKinnon, D. Jayatilaka, M.A. Spackman, Towards quantitative analysis of intermolecular interactions with Hirshfeld surfaces, Chem. Commun. (2007) 3814–3816.
[19] A. Gavezzotti, Calculation of Intermolecular Interaction Energies by Direct Numerical Integration over Electron Densities. I. Electrostatic and Polarization Energies in Molecular Crystals, J. Phys. Chem. B 106 (2002) 4145–4154.
[20] J.J. McKinnon, M.A. Spackman, A.S. Mitchell, Novel tools for visualizing and exploring intermol-ecular interactions in molecular crystals, Acta Crystallogr. B60 (2004) 627–668.
[21] D. Cremer, On the correct usage of the Cremer-Pople puckering parameters as quantitative descriptors of ring shapes - a reply to recent criticism by Petit, Dillen and Geise, Acta Crystallogr. B40 (1984) 498–500.
[22] D.G. Evans, J.C.A. Boeyens, Conformational analysis of ring pucker, Acta Crystallogr. B45 (1989) 581–590.
[23] G. Schiemenz, C. Näther, peri-Interactions in Naphthalenes, 7 [1]. A Hetera-naphthalene as a Model Compound for 8-Dimethylaminonaphth- 1-yl Silicon and Phosphorus Compounds, Zeitschrift für Naturforschung B 57 (3) (2002) 309–318.
[24] N.R. Sreenatha, B.N. Lakshminarayana, D.P. Ganesha, S. Vijayshankar, S. Nagaraju, Crystal Structure and Hirshfeld Surfaces of (*E*)-1-(2-Hydroxyphenyl)-3-(5-methylthiophen-2-yl)prop-2-en-1-one, X-ray Struct. Anal. Online 34 (2018) 23–24.
[25] S. Nagaraju, M.A. Sridhar, N.R. Sreenatha, C.S. Pradeepa Kumara, M.P. Sadashiva, Crystal Structure of (4-Fluorophenyl)(2-(methylthio)thiophen-3-yl)methanone, X-ray Struct. Anal. Online 34 (2018) 13–14.
[26] P. Braunstein, E. Cura, G.E. Herberich, Heterometallic complexes and clusters with 2-boratanaphthalene ligands, J. Chem. Soc. Dalton Trans. (11) (2001) 1754–1760.
[27] Said Daoui, Emine Berrin Cinar, Fouad El Kalai, Rafik Saddik, Khalid Karrouchi, Noureddine Benchat, Cemile Baydereb, Necmi Dege, Crystal structure and Hirshfeld surface analysis of 4-(4-methyl-benz-yl)-6-phenyl-pyridazin-3(2H)-one, Acta Crystallogr. E75 (2019) 1352–1356.
[28] Md. Serajul Haque Faizi, Emine Berrin Cinar, Onur Erman Dogan, Alev Sema Aydin, Erbil Agar, Necmi Dege, Ashraf Mashrai, Crystal structure, Hirshfeld surface analysis and DFT studies of 4-methyl-2-({[4-(tri-fluoro-meth-yl)phen-yl]imino}-meth-yl)phenol, Acta Crystallogr. E76 (2020) 1325–1330.
[29] Emine Berrin Cinar, Md. Serajul Haque Faizi, Nermin Kahveci Yagci, Onur Erman Dogan, Alev Sema Aydin, Erbil Agar, Necmi Dege, Ashraf Mashrai, Crystal structure, Hirshfeld surface analysis and DFT studies of (E)-4-methyl-2-{[(2-methyl-3-nitro-phen-yl)imino]-meth-yl}phenol, Acta Crystallogr. E76 (2020) 1551–1556.
[30] N.R. Sreenatha, B.N. Lakshminarayana, D.P. Ganesha, C.R. Gnanendra, S. Nagaraju, S. Madan Kumar, Structural and Hirshfeld surfaces of thiophene based isoxazole derivatives: 3-(3-Methylthiophen-2-yl)-5-(3,4,5-trimethoxyphenyl)isoxazole and 5-(3-Methylthiophen-2-yl)-3-(3,4,5-trimethoxyphenyl)isoxazole, Chem. Data Collect. 17–18 (2018) 394–403.
[31] N.R. Sreenatha, B.N. Lakshminarayana, D.P. Ganesha, C.R. Gnanendra, Crystal structure and Hirshfeld surface analysis of (*E*)-1-(3,5-di-chloro-2-hy-droxy-phen-yl)-3-(5-methyl-furan-2-yl)prop-2-en-1-one, Acta Crystallogr. E74 (2018) 1451–1454.
[32] Said Daoui, Emine Berrin Cinar, Necmi Dege, Tarik Chelfi, Fouad El Kalai, Abdulmalik Abudunia, Khalid Karrouchi, Noureddine Benchat, Crystal structure and Hirshfeld surface analysis of 4-(2,6-di-chloro-benz-yl)-6-[(E)-2-phenyl-ethen-yl]pyridazin-3(2H)-one, Acta Crystallogr. E77 (2021) 23–27.
[33] Semanur Yeşilbağ, Emine Berrin Çınar, Necmi Dege, Erbil Ağar, Eiad Saif, Crystal structure and Hirshfeld surface analysis of dimethyl 3,3′-{[(1*E*,2*E*)-ethane-1,2-diyl-idene]bis(aza-nylyl-idene)}bis-(4-methyl-benzoate), Acta Crystallogr. E78 (2022) 1–6.
[34] R. Jain, J.T. Ernst, O. Kutzki, H.S. Park, A.D. Hamilton, Protein recognition using synthetic surface-targeted agents, Mol. Divers. 8 (2014) 89–100.
[35] M.J. Turner, S.P. Thomas, M.W. Shi, D. Jayatilaka, M.A. Spackman, Energy frameworks: insights into interaction anisotropy and the mechanical properties of molecular crystals, Chem. Commun. 51 (2015) 3735–3738.
[36] N-R. Elejalde, E. Butassi, S. Zacchino, M.A. Macías, J. Portilla, Inter-molecular inter-action energies and molecular conformations in *N*-substituted 4-aryl-2-methyl-imidazoles with promising *in vitro* anti-fungal activity, Acta Crystallogr. B75 (2019) 1197–1207.
[37] N.R. Sreenatha, A.S. Harisha, D.P. Ganesha, T.N. Mahadeva Prasad, G.B. Thippeswamy, B.N. Lakshminarayana, Structural Investigation, Hirshfeld Surfaces and 3D Interaction Energy Analysis of the Compound 3-aryl-2-cyanoprop-2-enoic Acid, Eur. J. Appl. Phys. 4 (2022) 12–23.
[38] B.N. Lakshminarayana, N.R. Sreenatha, A.S. Jeevan Chakravarthy, B. Suchithra, S. Hariprasad, Structural, Computational and 3D Interaction Energy Calculations of the Compound 2-chloro-3-(1-napthyl)-5,5-dimethyl-2-cyclohexenone, Crystallogr. Rep. 67 (2) (2022) 201–208.
[39] Sumra Dilshad, Emine Berrin Çınar, Arif Ali, Adeeba Ahmed, Mohd Jane Alam, Musheer Ahmad, Aiman Ahmad, Necmi Dege, Eiad Saif, Crystal structure and Hirshfeld surface analysis of 2,4,6-tri-amino-pyrimidine-1,3-diium dinitrate, Acta Crystallogr. E78 (2022) 669–674.
[40] N.R. Sreenatha, A.S. Jeevan Chakravarthy, B.N. Lakshminarayana, S. Hariprasad, Structural characterization, computational, charge density studies of 2-chloro-3-(2'-methoxy)-5,5-dimethyl-2-cyclohexenone, J. Mol. Struct. 1225 (2021) 1–8.
[41] N.R. Sreenatha, A.S. Jeevan Chakravarthy, B. Suchithra, B.N. Lakshminarayana, S. Hariprasad, D.P. Ganesha, Crystal, spectral characterization, molecular docking, Hirshfeld computational studies and 3D-energy framework analysis of a novel puckered compound ($C_{14}H_{15}Cl$ O): 2-chloro-3-phenyl-5,5-dimethylcyclohex-2-en-1-one, J. Mol. Struct. 1210 (2020) 1–14.
[42] D.P. Ganesha, N.R. Sreenatha, C.R. Gnanendra, B.N. Lakshminarayana, Structural, Hirshfeld surface studies and computation of interaction energies of 4-Amino-N-(3-chloropyrazin-2-yl)benzene-1-Sulfonamide organic compound, Mater. Today Proc. 49 (2022) 817–823.
[43] C.F. Mackenzie, P.R. Spackman, D. Jayatilaka, M.A. Spackman, *CrystalExplorer* model energies and energy frameworks: extension to metal coordination compounds, organic salts, solvates and open-shell systems, IUCrJ 4 (5) (2017) 575–587.